



HAL
open science

A Bayesian technique for conditioning radar precipitation estimates to rain-gauge measurements

E. Todini

► **To cite this version:**

E. Todini. A Bayesian technique for conditioning radar precipitation estimates to rain-gauge measurements. Hydrology and Earth System Sciences Discussions, 2001, 5 (2), pp.187-199. hal-00304593

HAL Id: hal-00304593

<https://hal.science/hal-00304593>

Submitted on 18 Jun 2008

HAL is a multi-disciplinary open access archive for the deposit and dissemination of scientific research documents, whether they are published or not. The documents may come from teaching and research institutions in France or abroad, or from public or private research centers.

L'archive ouverte pluridisciplinaire **HAL**, est destinée au dépôt et à la diffusion de documents scientifiques de niveau recherche, publiés ou non, émanant des établissements d'enseignement et de recherche français ou étrangers, des laboratoires publics ou privés.

A Bayesian technique for conditioning radar precipitation estimates to rain-gauge measurements

Ezio Todini

Department of Earth and Geo-Environmental Sciences, University of Bologna, Italy
email: todini@geomin.unibo.it

Abstract

The paper introduces a new technique based upon the use of block-Kriging and of Kalman filtering to combine, optimally in a Bayesian sense, areal precipitation fields estimated from meteorological radar to point measurements of precipitation such as are provided by a network of rain-gauges. The theoretical development is followed by a numerical example, in which an error field with a large bias and a noise to signal ratio of 30% is added to a known random field, to demonstrate the potentiality of the proposed algorithm. The results analysed on a sample of 1000 realisations, show that the final estimates are totally unbiased and the noise variance reduced substantially. Moreover, a case study on the upper Reno river in Italy demonstrates the improvements in rainfall spatial distribution obtainable by means of the proposed radar conditioning technique.

Keywords: rainfall, meteorological radar, Bayesian technique, block-Kriging, Kalman filtering

Introduction

At present, there are essentially three basic systems for providing precipitation measurements for use in real-time flood forecasting.

The most common rain sensors for developing operational real-time flood forecasting systems are conventional ground-based telemetering rain-gauges, generally linked to a central station by telephone or radio links (VHF or UHF) or, less frequently, by Meteor-burst equipment or via satellite through Data Collection Platforms (DCPs). Several reasons favour conventional equipment based upon rain-gauges. First, they are the only ones that provide direct—albeit point—measurements of rainfall; second, national services have a tradition of using rain-gauges, so that long historical records are generally available for calibrating rainfall-runoff models; third, in real-time flood forecasting, there is a requirement for other ground-based hydrometeorological measurements, such as water levels in rivers and air temperatures close to the soil, sensors for which may be integrated into the overall data acquisition system so that the cost of additional rain sensors becomes marginal. Finally, in developing countries, training of local personnel and

maintenance is technically and economically more feasible with ground based equipment rather than with weather radars or satellites. The density of raingauge networks depends on several factors (WMO, 1981) and must be determined specifically for each case depending upon the orography and the spatial correlation of observations.

Another precipitation measurement system is the weather radar system, of growing importance in recent decades, particularly since the introduction of dual polarisation systems and Doppler radars. Over one hundred countries now operate 100s of weather radars and development programmes have also been established in several countries (Rosa Dias, 1994). The European Union sponsored COST72 (1985) and COST73 (Collier, 1990) for establishing a weather radar network in participating countries. In the USA, NEXRAD (1984) is a programme to establish a network of 175 S-band Doppler weather radars and, in the UK, the FRONTIERS programme combines radar and METEOSAT images to produce very short precipitation forecasts (Browning, 1979; Browning and Collier, 1982). There are two major benefits in using radars: a finer spatial description of the precipitation field can be obtained and approaching storms can sometimes be observed before they reach the

catchment of interest. A major disadvantage is the need for re-calibration of parameters used for converting reflectivity to rain; this generally requires the installation of a conventional ground-based rain-gauge network.

Until recently, meteorological radar systems have measured only reflectivity (usually indicated as Z). There is no simple correspondence between rain-rate (R) and reflectivity, so hundreds of different Z-R relationships are to be found in the literature. More recently multi-parameter radar rainfall algorithms have been introduced and Gorgucci *et al.* (2000) compared their performance.

A common practice in radar hydrology is, therefore, to calibrate the rain-rate derived using either the Z-R or the multi-parameter algorithms by means of rain-gauges: this is generally done using historical data. In real time, a different type of approach is taken, which involves the “adjustment” of the actual radar rain estimates on the basis of the rain-gauge measurements (Atlas *et al.*, 1997).

The third potentially useful measurement system is based upon the analysis of clouds shown by geo-stationary satellite images (Milford and Dugdale, 1989). This approach has been used successfully in tropical areas and, in particular, for the development of the Nile Flood Early Warning System (Grijzen *et al.*, 1992), but has not yet reached the quality required to implement operational flood forecasting systems on small or medium size catchments in sub-tropical areas.

Several techniques using meteorological radar/rain-gauge adjustment have been developed (also usable for satellite estimates): the spatial adjustment method, based upon an empirical negative exponential weighting, in its original formulation (Barnes, 1964; Brandes, 1975) involves the generation of a matrix of weights, or in slightly modified versions as proposed by Moore *et al.* (1989), Uijlenhoet *et al.* (1994); the domain adjustment technique (Collier *et al.*, 1983); the mean-field bias adjustment (Ahnert *et al.*, 1983; Lin and Krajewski, 1989); the radar-gauge coKriging (Creutin *et al.*, 1986; Krajewski, 1987, Seo *et al.*, 1990a,b).

Unfortunately, the coKriging technique is applicable only if one can actually compute the right-hand sides of a system of linear equations in terms of the covariances between true value of precipitation and both the gauge measurements and the radar estimates. This is obviously impossible because the true precipitation values are unknown. Krajewski (1987) approximated it on the basis of the radar covariance matrix but this is unsatisfactory since, unless the right-hand sides are known, the level of approximation of the final solution may become very large. A second problem relates to the co-Kriging constraints; in practice these require that, at each time-step, the total volume of rain must equal that estimated by the gauges, while the constraints should be set in a less rigid form on the expected values in time.

More recently, attention has been focused on multi-sensor merging using physically-based models (Lee and Georgakakos, 1990; Georgakakos and Krajewski, 1991; Seo and Smith, 1991a,b; French and Krajewski, 1994; French *et al.*, 1994).

While their conclusions on the effect of radar and rain-gauge combination are generally positive in terms of bias reduction (Borga *et al.*, 2000), they seem rather negative in terms of reduction of variance. In the case of uncertain covariance, Bayesian techniques have been used in Kriging for parameter estimation and the assessment of the uncertainty induced on the Kriging spatial functions (Kitanidis, 1986; Omre and Halvorsen, 1989; Le and Zidek, 1992; Handcock and Stein, 1993). A Bayesian formulation was used by Seo and Smith (1991a,b) to improve radar precipitation estimates by raingauge measurements, limiting their approach to the reduction of bias. In contrast, this paper introduces an original Bayesian combination technique that aims not only at eliminating the bias of meteorological radar precipitation estimates but also at producing minimum variance precipitation estimates on pixels of variable sizes ranging, for instance, from 1×1 to 10×10 km².

The first problem to be solved is that point measurements, such as are produced by rain-gauges, based upon a funnel of 1000 cm² catch area, cannot be compared directly to the average values of radar estimates over pixels of 1×1 km² or even larger. Hence, it is proposed to use block-Kriging to estimate the average field over the radar pixels and its variance from the point raingauge measurements.

The two estimates obtained from radar and rain-gauges are now comparable and, since it is reasonable to assume that they are independent estimates of the same unknown quantity, the effects of the two different estimation errors can be separated from their differences (Pereira Filho and Crawford, 1997).

Assuming that the rain-gauge estimates are unbiased, once the estimation error statistics have been determined, a Kalman Filter approach is taken to find the *a posteriori* estimates by combining the *a priori* estimates provided by the radar with the block-Kriged measurements provided by the gauges in a Bayesian framework.

Derivation of the proposed methodology

Given a random field y_i^R of precipitation on a lattice, which can be produced using radar (in real or in a log-transformed space), the problem of conditioning it to a set of point measurements, such as for instance the ones produced by rain-gauges, can be tackled as follows.

The first problem to be solved is that point measurements, such as those produced by rain-gauges that in the best case are based upon a funnel of 1000 cm² catch area, cannot be compared with average values of radar estimates over pixels of 1 km² or larger sizes. This inconsistency can be found for instance in Pereira Filho and Crawford's approach (1997), which uses the direct point differences between rain-gauges and radar estimates in a correction algorithm. In addition, the nature of their errors is quite different and complementary: rain-gauge measurements tend to be more accurate at a point while their spatial significance decays with distance and, hence, with area; in contrast, radar provides a better spatial (although biased) representation but a much poorer quantitative estimate.

To combine the two sets of data consistently, the first step is to regionalise the point rain-gauge measurements on a lattice made of pixels, on which the radar estimates are given, by means of block-Kriging and to estimate on this lattice the error statistics of the block-Kriged variables.

Rain-gauges, and in particular the most commonly used tipping-bucket rain-gauges, are relatively accurate instruments subject only to the so-called "volumetric" or "undercatchment" error, i.e. the fact that, at higher rain intensities, part of the water is not "weighed" by the tipping-bucket mechanism, thus violating the usual assumption that the volume of water needed to cause the bucket to tip is independent of the rainfall intensity. Nevertheless, Humphrey *et al.* (1997) and Lombardo and Staggi (1998), showed that this error is essentially a bias, with a small dispersion around it, that can be corrected, effectively, using the following (or similar calibration curves), with:

$$I = \alpha \cdot I_G^\beta \quad (1)$$

where:

- I is the actual rain intensity;
- I_G the rain-gauge measured intensity or the tipping rate (Niemczynowicz, 1986);
- α, β rain-gauge specific calibration parameters whose values are generally provided by the manufacturer and determined using special equipment such as the one described by Humphrey *et al.* (1997).

Other sources of error are due to evaporation that affects tipping bucket type gauges only at values smaller than their sensitivity, generally 0.2 mm using a standard WMO 1000 cm² funnel, (WMO, 1981), while errors due to wind effect can be reduced, but not totally eliminated, either by protective screens around the rain-gauge or by placing the rain-gauge at ground level, as proposed by the Institute of Hydrology, Wallingford. UK.

If one denotes the vector of n raingauge measurements at

time t , as x_t^G , a Kriging estimate of y_t^G on all the pixels of the lattice can be produced using the expression:

$$y_t^G = \Lambda x_t^G \quad (2)$$

where Λ , the $[m, n]$ matrix of weights, is obtained as:

$$[\Lambda \quad \mu] = [\Gamma_{lb} \quad u] \begin{bmatrix} \Gamma & \vdots & u \\ \cdots & \cdots & \cdots \\ u^T & \vdots & 0 \end{bmatrix}^{-1} \quad (3)$$

in which, with the usual Kriging notation Γ is the $[n, n]$ semi-variogram matrix among the n measurement points (the location of the rain-gauges), Γ_{lb} represents the $[m, n]$ semi-variogram matrix between the number of lattice squares m and the number of measured points n , u is an $[m]$ vector of ones and μ an $[m]$ vector of Lagrange multipliers. From the above discussion on error sources, the rain-gauge point measurements are considered unbiased, in that the bias can be corrected dynamically using Eqn. (1), while the measurement uncertainty can be accounted for, without formally changing Eqn. (3), by modifying the definition of the semi-variogram matrix, Γ , slightly, by subtracting from its principal diagonal the variance of the measurement errors, under the reasonable assumption of independence among errors affecting the different gauges (de Marsily, 1986).

Initially, Γ can be estimated from historical records on the assumption of second order stationarity in time of the rainfall field, for a given weather type, and updated as a function of the latest observations. Bayesian techniques, such as the one proposed by Omre and Halvorsen (1989) and Le and Zidek (1992) will be investigated for parameter estimation and parameter update.

Pereira Filho and Crawford (1997) pointed out that it is reasonable to assume that the two measurement systems, namely radar and rain-gauges, provide independent measures of the same unknown quantity. Therefore, their difference

$$\varepsilon_t = y_t^R - y_t^G \quad (4)$$

which, by adding and subtracting the true but unknown random field y_t , can also be written as:

$$\varepsilon_t = (y_t^R - y_t) - (y_t^G - y_t) \quad (5)$$

and can be used to assess the stochastic properties of the errors of estimate of the random field produced by the radar, by estimating its sample mean and its sample covariance. The statistical properties of ε_t can be expressed as:

$$E\{\varepsilon_t\} = \mu_{\varepsilon_t} = E\{y_t^R - y_t\} - E\{y_t^G - y_t\} = \mu_{\varepsilon_t^R} - \mu_{\varepsilon_t^G} \quad (6)$$

$$E\{(\varepsilon_t - \mu_{\varepsilon_t})(\varepsilon_t - \mu_{\varepsilon_t})^T\} = V_{\varepsilon_t} = E\left\{\left[(y_t^R - y_t) - \mu_{\varepsilon_t^R}\right]\left[(y_t^R - y_t) - \mu_{\varepsilon_t^R}\right]^T\right\} \\ + E\left\{\left[(y_t^G - y_t) - \mu_{\varepsilon_t^G}\right]\left[(y_t^G - y_t) - \mu_{\varepsilon_t^G}\right]^T\right\} = V_{\varepsilon_t^R} + V_{\varepsilon_t^G} \quad (7)$$

where the expected value (the bias) and the covariance matrix of ε_t are given as a function of the expected values and the covariances of ε_t^R and ε_t^G , namely the radar pixel average estimation error and the block-Kriged rain-gauge measurement error respectively. Bearing in mind that Kriging (as well as block-Kriging) is unbiased and allows for the estimation of the covariance matrix of the estimation errors, the following result may be verified easily:

$$\mu_{\varepsilon_t^G} = 0 \quad (8)$$

$$V_{\varepsilon_t^G} = \begin{bmatrix} \Lambda & \vdots & \mu \end{bmatrix} \begin{bmatrix} \Gamma & \vdots & u \\ \cdots & \cdots & \cdots \\ u^T & \vdots & 0 \end{bmatrix} \begin{bmatrix} \Lambda^T \\ \cdots \\ \mu^T \end{bmatrix} - \Gamma_{ll} \quad (9)$$

where Γ_{ll} is the $[m, m]$ semi-variogram matrix among all the reconstructed lattice squares. Thus by substituting Eqns. (8) and (9) into Eqns. (6) and (7), it is possible to estimate $\mu_{\varepsilon_t^R}$ and μ_{ε_t} as:

$$\mu_{\varepsilon_t^R} = \mu_{\varepsilon_t} \quad (10)$$

$$V_{\varepsilon_t^R} = V_{\varepsilon_t} - \left\{ \begin{bmatrix} \Lambda & \vdots & \mu \end{bmatrix} \begin{bmatrix} \Gamma & \vdots & u \\ \cdots & \cdots & \cdots \\ u^T & \vdots & 0 \end{bmatrix} \begin{bmatrix} \Lambda^T \\ \cdots \\ \mu^T \end{bmatrix} - \Gamma_{ll} \right\} \quad (11)$$

where μ_{ε_t} and V_{ε_t} can be estimated, from the time series of Eqn. (4), using a number of historical rainfall events. Additional research is needed for assessing the most appropriate technique for estimating μ_{ε_t} and V_{ε_t} : at the present time the estimation is based upon the assumption, for a given weather type, of second order stationarity in time of the differences ε_t given by Eqn. (4), while it is the intention of the writer to implement a Bayesian updating scheme for real time applications.

To combine the two sets of measurements (namely the block-Kriged point rain-gauge measurements and the radar lattice estimates) in a Bayesian way, one of the two random fields (in this paper, the one produced by the radar y_t^R) is taken as the *a priori* estimate and the other one (in this paper, that produced by the radar y_t^G), as the measurement vector

z_t , to give:

$$z_t = y_t^G = \Lambda x_t^G \quad (12)$$

Equation (12) can also be written in terms of the true but unknown field y_t to give:

$$y_t^G = y_t + (y_t^G - y_t) \quad (13)$$

or, using the standard Kalman filter notation:

$$z_t = H_t y_t + \eta_t \quad (14)$$

After substituting in Eqn. (13)

$$\eta_t = y_t^G - y_t \quad (15)$$

and setting

$$H_t = I \quad (16)$$

Equation (14) can now be considered as the measurement equation of a classical Kalman filter (Kalman, 1960; Kalman and Bucy, 1961) in which:

$$E\{\eta_t\} = \mu_{\eta_t} = E\{y_t^G - y_t\} = \mu_{\varepsilon_t^G} = 0 \quad (17)$$

$$E\{\eta_t \eta_t^T\} = V_{\eta_t} = E\left\{\left[(y_t^G - y_t) - \mu_{\varepsilon_t^G}\right]\left[(y_t^G - y_t) - \mu_{\varepsilon_t^G}\right]^T\right\} = V_{\varepsilon_t^G} \\ = \begin{bmatrix} \Lambda & \vdots & \mu \end{bmatrix} \begin{bmatrix} \Gamma & \vdots & u \\ \cdots & \cdots & \cdots \\ u^T & \vdots & 0 \end{bmatrix} \begin{bmatrix} \Lambda^T \\ \cdots \\ \mu^T \end{bmatrix} - \Gamma_{ll} \quad (18)$$

At this point, by taking

$$y_t' = y_t^R - \mu_{\varepsilon_t^R} \quad (19)$$

as the *a priori* estimate of the state and

$$P_t' = V_{\varepsilon_t^R} \quad (20)$$

as the *a priori* estimate of its covariance matrix, it is possible

to compute the innovation v_t as:

$$v_t = z_t - H_t y_t' = \Lambda x_t^G - y_t^R + \mu_{\varepsilon_t^R} \quad (21)$$

and the Kalman gain K_t as:

$$K_t = P_t' (P_t' + V_{\eta_t})^{-1} = V_{\varepsilon_t^R} (V_{\varepsilon_t^R} + V_{\varepsilon_t^G})^{-1} = V_{\varepsilon_t^R} V_{\varepsilon_t^G}^{-1} \quad (22)$$

Finally, the Kalman Filter equations allow the *a posteriori* estimate to be found by combining the *a priori* estimate and the measurements in a Bayesian framework to give:

$$y_t'' = y_t' + K_t v_t = y_t^R - \mu_{\varepsilon_t^R} + V_{\varepsilon_t^R} V_{\varepsilon_t^G}^{-1} (\Lambda x_t^G - y_t^R + \mu_{\varepsilon_t^R}) \quad (23)$$

$$P_t'' = P_t' - K_t H_t P_t' = V_{\varepsilon_t^R} - V_{\varepsilon_t^R} V_{\varepsilon_t^G}^{-1} V_{\varepsilon_t^R} \quad (24)$$

where y_t'' is the *a posteriori* estimate of the random field over the lattice and P_t'' its error of estimate covariance matrix. The solution proposed by Eqn. (23) is not limited to a radar bias correction, as in Ahnert *et al.*, 1986; on the contrary, the proposed technique offers a multivariate Bayesian combination of radar estimates and rain-gauge measurements on the basis of the local relative uncertainty. Finally, the developed Kalman filter is based upon a “static” formulation in which the time evolution of the measurement error structure is not taken into account. Further improvements to the proposed methodology, requiring real-time updates of the means and covariance matrices as a function of their time evolution, will be tested in the future.

A numerical example

Because the true rainfall field is unknown in real-world applications, it was felt necessary to demonstrate the effectiveness of the proposed methodology in terms of the *a posteriori* estimates convergence towards the true, but supposed unknown values, by means of a numerical example.

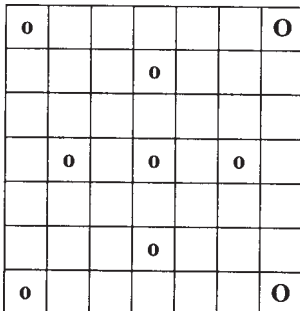


Fig. 1. The lattice and the location of the gauges

In the proposed example, the radar measurements are assumed to be available on a 7×7 lattice with sides of 1000 m, while nine rain-gauges are assumed to be set in the centres of the lattice cells, as in Fig. 1.

A Gaussian random field y_t , taken as the true field, is then generated jointly on the lattice and on the measurement points, for 1000 time-steps, with the following covariance

$$V_{y_t}(h) = \sigma^2 - \left[p + \omega \left(1 - e^{-h^2/a} \right) \right] \quad \text{and parameters as in Table 1.}$$

Table 1. Random field parameters

Mean (μ)	Variance (σ^2)	Nugget (p)	Sill (ω)	Range (a)
0	10,000	0	10,000	10^7

This generation involved the computation of the following covariance matrix:

$$BB^T = \begin{bmatrix} \Gamma_{ll} & \vdots & \Gamma_{lb} \\ \dots & \dots & \dots \\ \Gamma_{bl} & \vdots & \Gamma \end{bmatrix} \quad (25)$$

and the derivation of its square root B by the eigenvalue-eigenvector decomposition and the generation of the process vector at each time interval, namely:

$$\begin{bmatrix} y_l \\ \dots \\ y_b \end{bmatrix}_t = B \begin{bmatrix} \delta_l \\ \dots \\ \delta_b \end{bmatrix}_t \quad (26)$$

where δ_l, δ_b are $49+9$ NIP(0,1) variables.

In the example, the rain-gauge point measurements are considered unaffected by measurement errors, while the radar estimates are considered biased and affected by noise. Therefore, 1000 time realisations of a Gaussian random noise were generated with the parameters given in Table 2.

Table 2. Random noise field parameters

Mean (μ)	Variance (σ^2)	Nugget (p)	Sill (ω)	Range (a)
40	3,000	0	3,000	10^6

The noise was then added to the “true” value $[y_l]_t$ to give the noise corrupted observations y_t^R similar to the ones one could expect from a radar. In practice, the error represents a very large bias and a variance of the order of 30% of the signal. The data used for the analysis were then the 1000 sets of 49 noise corrupted “radar” estimates on the lattice

and the corresponding 1000 sets of nine perfect point “raingauge” measures.

To show the efficiency of the proposed procedure, it was applied on the assumption that the random field parameters were known, so that no estimation error was involved in the process.

Through application of the Kalman Filter Eqn. (23), 1000 sets of 49 *a posteriori* estimates were obtained. The “true” field was then subtracted both from the *a priori* as well as from the *a posteriori* estimates and the statistics were computed for all the lattice cells.

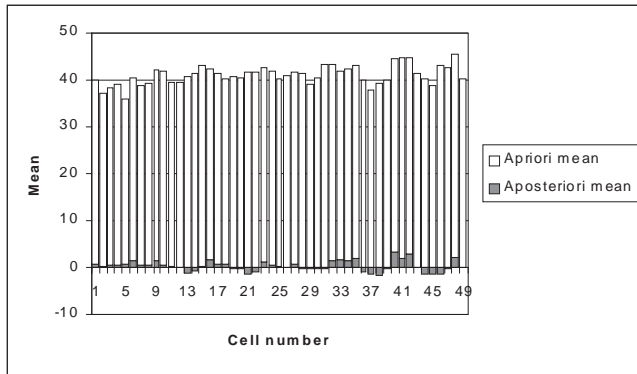


Fig.2. Bias reduction in the 49 lattice cells

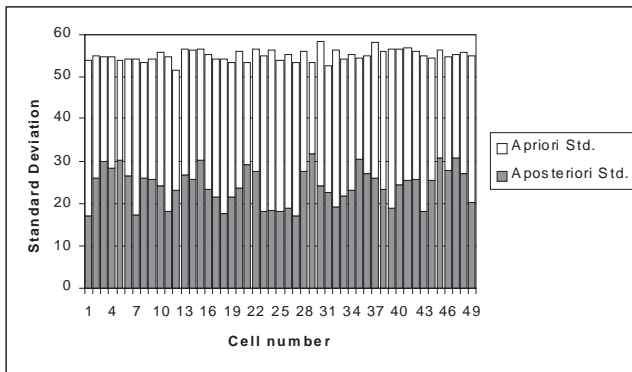


Fig. 3. Standard deviation reduction in the 49 lattice cells

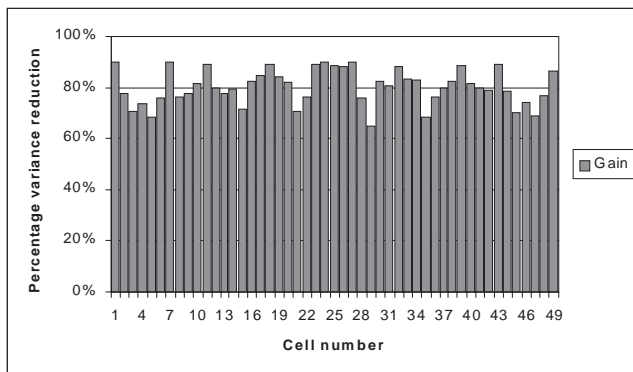


Fig. 4. Percentage variance reduction (gain) for the 49 cells

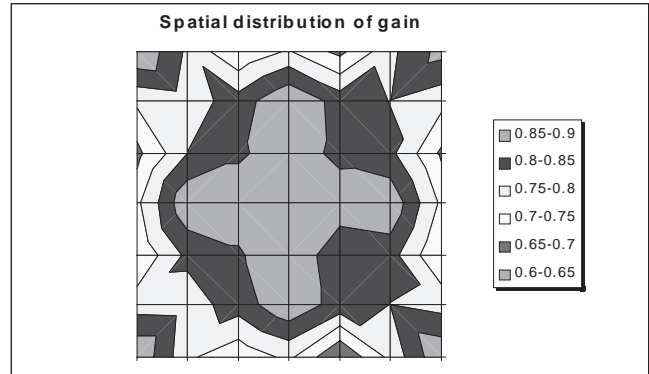


Fig. 5. Spatial distribution of the percentage variance reduction

Although dealing with purely Gaussian fields where the methodology is by definition “optimal”, the results are nonetheless impressive. The bias has been totally eliminated over the entire lattice (Fig. 2), while Fig. 3 shows that the standard deviation of errors has been more or less halved. Figure 4 shows the variance gain, namely the percentage reduction in variance, which varies between 90% and 65% as a function of the distance from the rain-gauges and from the centre as is shown in Fig. 5 where the gain is plotted for the different cells.

The proposed method performs far better than the empirical negative exponential weighting used by Brandes (1975), for which no bias elimination and no minimum variance weighting parameter estimation is applied, leaving the parameter choice to subjective judgement.

Finally, it is not expected that the estimation of the Kriging parameters will modify strongly the results obtained, given their small influence on the estimation of the covariance matrix, for which a decent approximation produces good results.

The case study

To analyse the performance of the proposed methodology on real-world data, a case study was set up on the upper Reno river close to Casalecchio, near Bologna (Italy), where several rain-gauges and a meteorological radar are available.

The river catchment has a surface area of 1051 km² and ranges in elevation from 0 to 2000 m, as shown by the Digital Terrain Model in Fig. 6. Combined with the prevailing extension of clayey and marly soils, with a few alluvial deposits in its terminal section, the catchment gives rise to flood waves that can reach 1900 m³ s⁻¹.

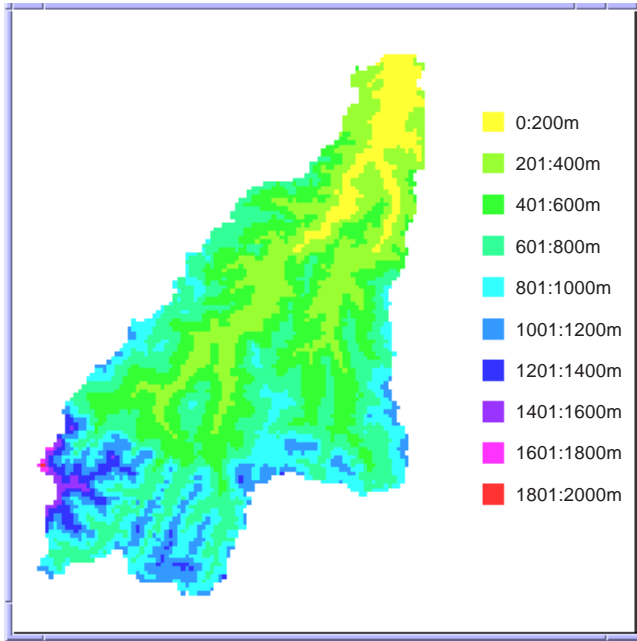


Fig. 6. The Digital Terrain Model (DTM) of the upper Reno River

AVAILABLE DATA

The Regional Meteorological Service provides hourly maps of rainfall estimated by a C-band Doppler radar is located about 30 km north-east of Casalecchio, in the Po Valley; its main characteristics are given in Table 3. A double polarisation radar like the one available, emits electromagnetic impulses polarised in orthogonal directions, measuring the differential reflectivity Z_{DR} , that is the difference between reflectivity values in the two different polarisation (Z_H, Z_V horizontal and vertical) directions:

$$Z_{DR} = 10 \log \left(\frac{Z_H}{Z_V} \right) \quad (27)$$

Radar data are obtained from reflectivity volumetric measures with 250 m range resolution for several elevations ($0,5^\circ, 1,4^\circ, 2,3^\circ$) and azimuths. The composite reflectivity PPI (Plan Position Indicator) maps are constructed by averaging spatially over cells of $1 \times 1 \text{ km}^2$ and, depending on the orography, at any azimuth and range the first PPI not

Table 3. The meteorological radar characteristics

Managing agency	Regione Emilia-Romagna
Site (denomination, lat., long.)	S.Pietro Capofiume $44^\circ 39'$, $-0^\circ 50'$
Height a.s.l.	11 m
Capability	Doppler Double Polarisation
Band	C
Wavelength	5.5 cm
Processing	digital
Antenna	
Beam width	0.9
Polarisation	horizontal
Gain	>45 dB
Scanning method	volumetric, sectorial
Transmitter/Receiver	
Frequency	5450-5650 MHz
Type	klystron
Pulse length and ass. PRF	0.5, 1.5, 3.0 ms –1200, 600, 300 Hz
Receiver type	Log and Lin
Band Log. dynamic range	80 dB
Band Lin. dynamic range	from 30 dB to 90 dB with I.A.G.C.
RSP/RDP	
Range bin	125, 250, 500 m - 1 km
Covering Range	125, 250 km
Possible resolutions	125 m at 125 km, 250 m at 250 km
Range	
Possible diff. op. outputs	CAPPI Z, Z_{DR} , v, s_v , HVMI
Scan strategy	every 5 min. vol. acquisition
Max height of RDP outputs	16 km

considerably affected by the ground echoes (clutter) is retained. Furthermore, an algorithm able to eliminate anomalous propagation echoes is also running at the Regional Meteorological Service.

The $1 \times 1 \text{ km}^2$ maps are collected every 15 minutes and converted into rainfall intensity by means of the classical Marshall and Palmer relationship and the rainfall intensities are then averaged to obtain hourly cumulative rainfall data.

Several recording rain-gauges are also available in the upper Reno river catchment. Table 4 provides a list of the 26 gauges used in the case study together with their geographical position and the elevation in metres a.s.l.

Table 4. List of rain gauge stations in the upper Reno river basin

<i>n</i>	<i>Gauging station</i>	<i>LAT.</i> ⁽¹⁾	<i>LON.</i> ⁽²⁾	<i>Elevation</i> (m a.s.l.)
1	Piastre	44°03'	1°31'	741
2	Maresca	44°04'	1°36'	1,043
3	Pracchia	44°03'	1°32'	627
4	Orsigna	44°05'	1°34'	806
5	Monte Pidocchina	44°04'	1°31'	1,100
6	Diga di Pavana	44°07'	1°27'	480
7	Porretta Terme	44°09'	1°28'	349
8	Monteacuto delle Alpi	44°08'	1°34'	915
9	Lizzano in Belvedere	44°09'	1°33'	640
10	Bombiana	44°13'	1°29'	804
11	Acquerino	44°00'	1°26'	890
12	Treppio	44°05'	1°25'	710
13	Diga di Suviana	44°08'	1°25'	500
14	Riola di Vergato	44°13'	1°23'	240
15	Vergato	44°17'	1°20'	195
16	Cottede	44°07'	1°16'	850
17	Diga del Brasimone	44°07'	1°20'	830
18	Monteacuto Vallese	44°14'	1°15'	747
19	Monzuno	44°16'	1°11'	620
20	Sasso Marconi	44°23'	1°13'	130
21	Montepastore	44°22'	1°20'	596
22	Monte San Pietro	44°22'	1°05'	317
23	Bologna San Luca	44°29'	1°09'	286
24	Monghidoro	44°13'	1°08'	841
25	Pianoro	44°22'	1°06'	187
26	Traversa	44°06'	1°10'	871

⁽¹⁾ 1' in latitude is equal to 1850 m.

⁽²⁾The longitude refers to the Rome Meridian (Monte Mario). The longitude of Monte Mario in relation to Greenwich is 12°27'08"

1' in longitude is equal to 1330 m.

The case study refers to the eight days from 4–11 November, 1994. This event was chosen because of anomalous radar precipitation estimates. This anomaly can be detected from Fig. 7, where the discharges measured at Casalecchio (thick black line) are compared to those estimated by a rainfall-runoff model using alternatively: (1) the precipitation obtained by Kriging the point rain-gauge measures (thin grey line) or (2) the radar estimated rainfall (thick grey line), as the input to the model. While the first part of the flood event is reproduced well using both areal rainfall estimates produced by the rain-gauges and the radar, the second part is reproduced only by the gauges, while the radar underestimate the rain intensity over the catchment. The cause of this anomaly can neither be interpreted as a lack of radar calibration, because radar performed quite well during the first portion of the event nor as a consequence of radar failures (Fig. 8 shows the period of radar failures), which happened on 46 of the 192 hours, luckily during either dry or very light rain spells.

In summary, the following data were available for the case study:

- (1) 146 hours of radar precipitation estimates at 1084 pixels of $1 \times 1 \text{ km}^2$;
- (2) The geographical co-ordinates of the 1084 pixels;
- (3) 192 hours of rain-gauge precipitation measurements at 26 locations;
- (4) The geographical co-ordinates of the 26 rain-gauge locations;

ESTIMATION OF SEMI-VARIOGRAM AND RELEVANT PARAMETERS

Following the procedure proposed, the first step is to apply block-Kriging to the point rain-gauge measurements, which requires the estimation of the semi-variogram, and relevant parameters, from the 26 rain-gauge measurements.

Several hours of rainfall measurements were available, so the semi-variogram was not estimated by using the classical Kriging approach which takes into consideration a unique set of measures in time: rather, the semi-variogram was derived from an estimate of the covariance matrix, which was based on all the available data in space and time. Moreover, given that several time intervals were dry, not all the 192 available measurement hours were used to estimate the spatial correlation; hourly measurements showing no rain in more than five gauges were rejected: this reduced the 192 hours of measurement to only 47.

Once the covariance matrix is available, the semi-variogram value can be computed from its definition as:

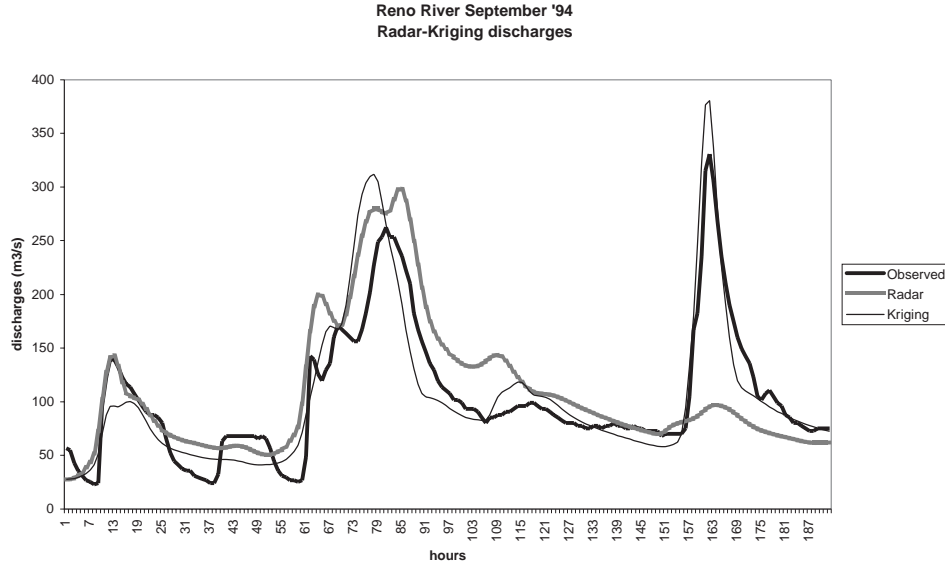


Fig. 7. Discharges measured at Casalecchio (thick black line) and estimated using the Kriged point rain-gauge measures (thin grey line) or the radar estimated rainfall (thick grey line)

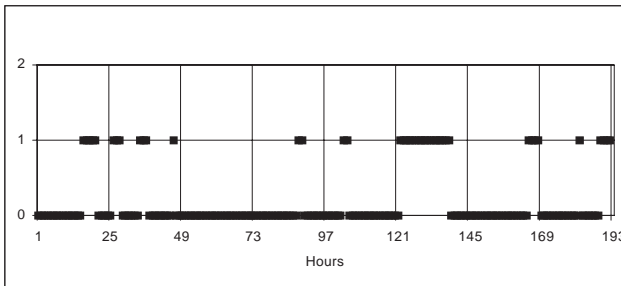


Fig. 8. Periods of available (0) and missing (1) radar data

$$\gamma(h_{i,j}) = \frac{1}{2} [Cov(i,i) + Cov(j,j) - 2 \cdot Cov(i,j)] \quad (28)$$

where $h_{i,j}$ is the distance between the two rain-gauges i and j .

The semi-variogram model and its parameter values can then be estimated in the classical way by dividing the maximum distance among the rain-gauges in classes (in this case 5000 m distance classes were used), by computing the average value per class and by fitting the different models as a function of their parameter values.

In the proposed case, the best results were obtained using the Gaussian semi-variogram, given in Eqn. (29) as a function of its three parameters, p the nugget, ω the sill and a the range:

$$\gamma(h) = p + \omega \left(1 - e^{-(h/a)^2} \right) \quad (29)$$

Table 5. Gaussian semi-variogram parameter value estimates

Nugget (p)	Sill (ω)	Range (a)
2.66	1148	951048

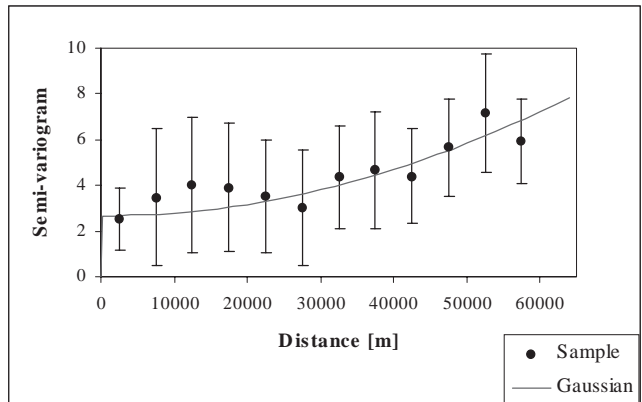


Fig. 9. Gaussian semi-variogram compared to sample estimates $\pm 2\sigma$ limits

The parameter values obtained are given in Table 5, while Fig. 9 compares the sample estimates, plus or minus two sigma limits, and the estimated Gaussian semi-variogram.

ESTIMATION OF BLOCK SEMI-VARIOGRAMS

The application of the proposed methodology, based upon the block-Kriging and the Kalman Filter, requires the estimation of the following matrices which contain the semi-variogram values computed among gauges (Γ), among gauges and radar pixels (Γ_{lb}), among radar pixels (Γ_{ll}).

In the proposed case study, the matrix Γ is the symmetrical $[n+1, n+1]$ matrix, with $n=26$ the number of gauges, defined as:

$$\Gamma = \begin{bmatrix} 0 & \gamma_{12} & \gamma_{13} & \dots & \gamma_{1n} & 1 \\ \gamma_{21} & 0 & \gamma_{23} & \dots & \gamma_{2n} & 1 \\ \gamma_{31} & \gamma_{32} & 0 & \dots & \gamma_{3n} & 1 \\ \dots & \dots & \dots & \dots & \dots & 1 \\ \gamma_{n1} & \gamma_{n2} & \gamma_{n3} & \dots & 0 & 1 \\ 1 & 1 & 1 & \dots & 1 & 0 \end{bmatrix} \quad (30)$$

where $\gamma_{i,j} = \gamma(h_{i,j})$ is computed using Eqn. (29).

The matrix Γ_{lb} is the $[m, n+1]$ matrix, with $m=1084$ the number of radar pixels, defined as:

$$\Gamma_{lb} = \begin{bmatrix} \bar{\gamma}_{11} & \bar{\gamma}_{12} & \dots & \bar{\gamma}_{1n} & 1 \\ \bar{\gamma}_{21} & \bar{\gamma}_{22} & \dots & \bar{\gamma}_{2n} & 1 \\ \bar{\gamma}_{31} & \bar{\gamma}_{32} & \dots & \bar{\gamma}_{3n} & 1 \\ \dots & \dots & \dots & \dots & \dots \\ \dots & \dots & \dots & \dots & \dots \\ \bar{\gamma}_{m1} & \bar{\gamma}_{m2} & \dots & \bar{\gamma}_{mn} & 1 \end{bmatrix} \quad (31)$$

where $\bar{\gamma}_{i,j}$ is estimated, according to Eqn. (32) as the average over pixel j of the semi-variogram from point i :

$$\bar{\gamma}_{i,j} = \frac{\int_{x_j} \int_{y_j} \gamma \left[\sqrt{(x_i - \xi)^2 + (y_i - \eta)^2} \right] d\xi d\eta}{\int_{x_j} \int_{y_j} d\xi d\eta} \quad (32)$$

The matrix Γ_{ll} is the symmetrical $[m, m]$ matrix, defined as:

$$\Gamma_{ll} = \begin{bmatrix} \bar{\bar{\gamma}}_{11} & \bar{\bar{\gamma}}_{12} & \dots & \bar{\bar{\gamma}}_{1m} \\ \bar{\bar{\gamma}}_{21} & \bar{\bar{\gamma}}_{22} & \dots & \bar{\bar{\gamma}}_{2m} \\ \bar{\bar{\gamma}}_{31} & \bar{\bar{\gamma}}_{32} & \dots & \bar{\bar{\gamma}}_{3m} \\ \dots & \dots & \dots & \dots \\ \bar{\bar{\gamma}}_{m1} & \bar{\bar{\gamma}}_{m2} & \dots & \bar{\bar{\gamma}}_{mm} \end{bmatrix} \quad (33)$$

where

$$\bar{\bar{\gamma}}_{i,j} = \frac{\int_{x_i} \int_{y_i} \int_{x_j} \int_{y_j} \gamma \left[\sqrt{(x_i - \xi)^2 + (y_i - \eta)^2} \right] d\xi d\eta d\chi d\zeta}{\int_{x_i} \int_{y_i} \int_{x_j} \int_{y_j} d\xi d\eta d\chi d\zeta} \quad (34)$$

The integrals appearing in Eqns. (32) and (34) can be computed easily for the Gaussian model since an analytical expression can be derived for squared or rectangular pixels, while numerical estimates must be used for most of the other semi-variogram types and integration domains.

The matrices of Eqns. (30), (31) and (32) are exclusively a function of the semi-variogram as well as of the coordinates of the rain-gauges and of the radar pixels; therefore, they are kept unchanged as a function of rainfall data. This implies the assumption of weak stationarity in time for the first and second moments of the rainfall process. When a unique weather type is driving the rainfall event, as in the present case study, this hypothesis seems reasonable. Nevertheless, further investigation must be carried out to assess the effect of changes in the spatial covariance (as well as in the semi-variogram) structure as a function of changed weather type conditions, which would recommend the use of different estimates according to the specified weather type.

APPLICATION RESULTS

Once the matrices were estimated, the block-Kriging Bayesian correction technique was applied to the 146 available contemporary rain-gauge and radar measurements. As opposed to the earlier numerical example, in the real-world case study, the true value of the precipitation over each pixel is unknown, which means that the actual variance reduction cannot be estimated. Nevertheless, it is possible to evaluate the reduction of bias and of time variance between y_t^G , the block-Kriged rainfall, derived from the rain-gauges, and y_t'' , the *a posteriori* estimate, by computing the difference $(y_t^G - y_t'')$ and by estimating its expected value and covariance matrix. Given the large size of the matrices $[1084 \times 1084]$ and vectors $[1084]$ involved, an overall measure of results will be given by averaging in space over the 1084 pixels the resulting performances.

Table 6. Bias and variance reduction

Variable	<i>A priori</i> $(y_t^G - y_t')$	<i>A posteriori</i> $(y_t^G - y_t'')$
Bias	0.34	0.07
Variance	11.29	1.87

While, on the assumption that the block-Kriging is unbiased, the bias reduction is actually representative of the improvements, the variance reduction must be considered cautiously. As discussed earlier, y_t^G and y_t' can be assumed independent but this is not true for y_t^G and y_t'' since the *a posteriori* estimate incorporates the information brought by

the measurement. Therefore, taking into account the fact that the two series are not independent, part of the large reduction obtained in the overall variance is due to the increased correlation between the time pattern of the two time series, which is itself a beneficial property.

This was not so in the previous numerical simulation example, where y_t the “true” value of precipitation was known and used to measure the reduction in variance from $Var(y'_t - y_t)$ to $Var(y''_t - y_t)$, which is why it was felt essential for the completeness of this research.

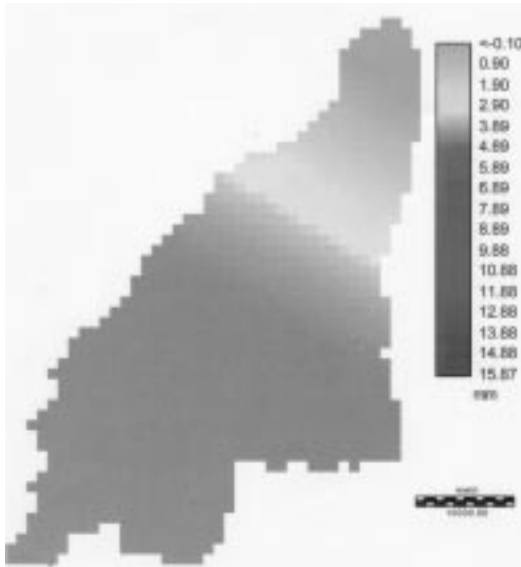


Fig. 10. *Block Kriged rain-gauges*

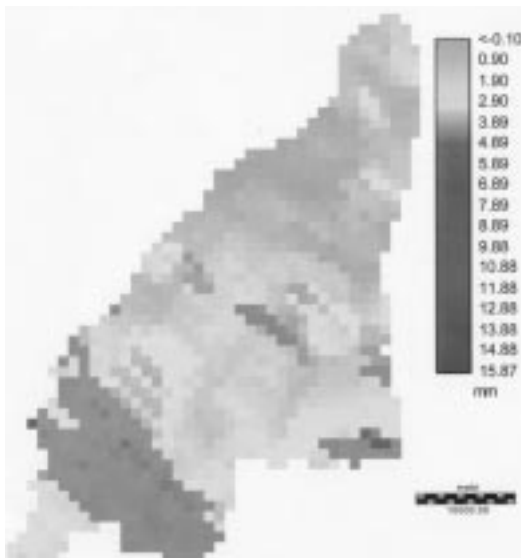


Fig. 11. *Radar rain estimates*

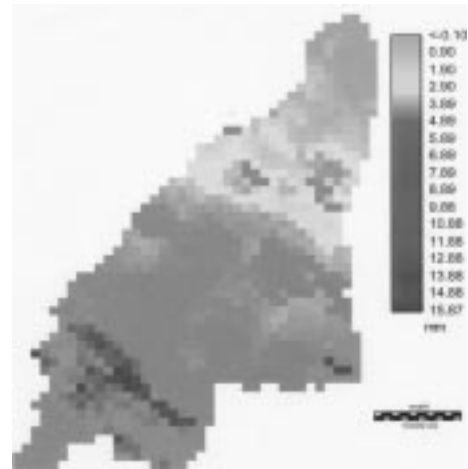


Fig. 12. *Bayesian combination*

In a more qualitative manner, the results of the case study can be discussed by looking at Figs. 10, 11 and 12 which show the effect of the proposed method during the anomalous behaviour of the radar. The figures refer to the 160th hour. Figure 10 shows the smoothed surface, produced by block-Kriging, of the rainfall intensities increasing from the northern lower edge to the upstream southern mountain part of the catchment. Figure 11 shows what was estimated on the basis of the radar data: there was a heavy rainstorm in the upper part of the catchment, with practically no rain anywhere else. Figure 12, the Bayesian combination, extends the amount of rainfall estimated by the radar to the other portions of the catchment, while preserving the spatial variability. This does not mean that this is the true rainfall: this is only a more likely estimate in which the uncertainty in the different measurement methods has been reduced successfully.

Conclusions and further work

The new block-Kriging-Bayesian technique for combining weather radar based rainfall estimates with rain-gauge measurements is open to a wide range of possible applications. The technique is needed particularly for real-time flood forecasting applications where the reliability and the reduction of uncertainty are the major requirements. To this end, it is expected that the proposed methodology will increase the credibility of the radar based rainfall estimates.

The test on numerical data has demonstrated the efficiency of the technique and application to real-world data has given qualitative confirmation of the improvements that can be obtained by its application.

To complete the development of the block-Kriging-

Bayesian approach, further tests and analyses will be performed within the frame of MUSIC. These will deal with the comparison of the proposed technique with the co-Kriging radar-rainfall approach of Krajewski (1987); the analysis of the relevance of the rain gauge measurement errors; the assessment of the effects of time variations in the rainfall spatial co-variance structure as a function of the different weather types and the possibility of a Bayesian update for their estimates.

Nonetheless, extensive application of the technique is anticipated within the frame of a recently approved EU-funded project MUSIC (Multi Sensor precipitation measurements Integration, Calibration and flood forecasting) where, in addition, a combination of three different measurement systems (weather radar, satellite and rain-gauges) will be tested for the benefit of all possible sources of independent information.

References

- Ahnert, P.R., Hudlow, M.D., Greene, D.R. and Johnson, E.R., 1983. Proposed on site precipitation processing system for NEXRAD. *Preprint, 21st Conference on Radar Meteorology*, Edmonton, Alberta, Canada.
- Ahnert, P.R., Krajewski, W.F. and Johnson, E.R., 1986. Kalman filter estimation of radar-rainfall field bias, *Preprint, 23rd Conference on Radar Meteorology, American Meteorol. Soc.*, JP 33-37.
- Atlas, D., Ryzhkov, A. and Zrnic, D., 1997. Polarimetrically tuned Z-R relations and comparison of radar rainfall methods. In: *Weather Radar Technology for Water Resources Management*, B. Braga Jr. and O. Massambani (Eds.). UNESCO Press, Paris, France, 3–67.
- Barnes, E.A., 1964. A technique for maximising details in numerical weather map analysis. *J. Appl. Meteorol.*, **3**, 396–409.
- Borga, M., Anagnostou, E.N. and Frank, E., 2000. On the use of real-time radar rainfall estimates for flood predictions in mountainous basins. *J. Geophys. Res.* **105**, 2269–2280.
- Brandes, E.A., 1975. Optimizing Rainfall Estimates with the Aid of Radar. *J. Appl. Meteorol.*, **14**, 1339–1345.
- Browning, K.A., 1979. The FRONTIERS plan: a strategy for using radar and satellite imagery for short range precipitation forecasting. *Meteorol. Mag.*, **108**, 161–184.
- Browning, K.A. and Collier, C.G., 1982. An integrated radar-satellite nowcasting system in the UK. In: *Nowcasting*, Browning K.A. (Ed.). Academic Press, London, 47–61.
- Collier, C.G., Larke, P.R. and May, B.R., 1983. A weather radar correction procedure for real-time estimation of surface rainfall. *Quart. J. Roy. Meteorol. Soc.*, **109**, 589–608.
- Collier, C.G., 1990. COST 73: The development of a weather radar network in Western Europe. In: *Weather Radar Networking Seminar on COST Project 73*, C.G. Collier and M. Chapuis (Eds.). Kluwer Academic Publishers, Netherlands, EUR 12414 EN - FR.
- COST Project 72, 1985. *European Commission Report EUR 10353 EN - FR*.
- Creutin, J.D., Delrieu, G. and Lebel, T., 1986. Rain measurement by raingauge-radar combination: a geostatistical approach. *J. Appl. Atmos. Ocean. Technol.*, **5**, 102–115.
- de Marsily, G., 1986. *Quantitative Hydrogeology*, Academic Press.
- French, M.N. and Krajewski, W.F., 1994. A model for real time rainfall forecasting using remote sensing, 1, Formulation. *Water Resour. Res.*, **30**, 1075–1083.
- French, M.N., Andrieu, H. and Krajewski, W.F., 1994. A model for real time rainfall forecasting using remote sensing, 2, Case Studies. *Water Resour. Res.*, **30**, 1085–1094.
- Georgakakos, K.P. and Krajewski, W.F., 1991. Worth of radar data in the real time prediction of mean areal rainfall by non-advective physically based models. *Water Resour. Res.*, **27**, 185–197.
- Gorgucci, E., Sarchilli, G. and Chandrasekar, V., 2000. Sensitivity of multiparameter radar rainfall algorithms. *J. Geophys. Res.* **105**, 2215–2223.
- Grijzen, J.G., Snoeker, X.C., Vermeulen, C.J.M., Mohamed El Amin Moh. Nur and Yasir Abbas Mohamed, 1992. An information system for flood early warning. In: *Floods and Flood Management*, A.J. Saul (Ed.). Kluwer Academic Publishers, 263–289.
- Handcock, M.S. and Stein, M.L., 1993. A Bayesian analysis of Kriging. *Technometrics*, **35**, 403–410.
- Humphrey, M.D., Istok, J.D., Lee, J.Y., Hevesi, J.A. and Flint, A., 1997. A new method for automated dynamic calibration of tipping-bucket rain gauges. *J. Atmos. Ocean. Technol.*, **14**, 1513–1519.
- Kalman, R.E., 1960. A new approach to linear filtering and prediction problems. *A.S.M.E. J. Basic Eng. Series*, **82**, 35–45.
- Kalman, R.E. and Bucy, R.S., 1961. New results in linear filtering and prediction theory. *A.S.M.E. J. Basic Eng. Series*, **83**, 85–108.
- Kitanidis, P.K., 1986. Parameter uncertainty in estimation of spatial functions: Bayesian analysis. *Water Resour. Res.*, **22**, 499–507.
- Krajewski, W.F., 1987. Co-kriging radar-rainfall and raingage data, *J. Geophys. Res.*, **92**, 9571–9580.
- Le, N.D. and Zidek, J.V., 1992. Interpolation with uncertain spatial covariances: a Bayesian alternative to Kriging. *J. Multivariate Anal.*, **43**, 351–374.
- Lee, T.H. and Georgakakos, K.P., 1990. A two-dimensional stochastic dynamic quantitative precipitation forecasting model. *J. Geophys. Res.*, **95**, 2113–2126.
- Lin, D.S. and Krajewski, W.F., 1989. Recursive methods of estimating Radar-rainfall field bias. *Preprint, 24th Conference on Radar meteorology*, Tallahassee, Florida, USA.
- Lombardo, F. and Staggi, L., 1998. Verifica e taratura dinamica della strumentazione pluviometrica finalizzata alla valutazione degli errori per intensità di pioggia elevata, *Proc. XXVI Convegno di Idraulica e Costruzioni Idrauliche*, **II**, 85-96 (in Italian).
- Milford, J.R. and Dugdale, G., 1989. Estimation of rainfall using geostationary satellite data. *Applications of Remote Sensing in Agricultural Sciences*, University of Nottingham, Butterworth, London.
- Moore, R.J., Watson, B.C., Jones, D.A., Black, K.B., Haggett, M.A., Crees, M.A. and Richard, C., 1989. Towards an improved system for weather radar calibration and rainfall forecasting using raingauge data from a regional telemetry system. In: *New directions for surface water modelling*, Proc. 3rd Scientific Assembly IAHS, M.L. Kavvas (Ed.). IAHS Publication no. 181, 13-21.
- NEXRAD, 1984. *Next Generation Weather Radar, Programmatic Environmental Impact Statement R400-PE201*, NEXRAD Joint System Program Office, US Dept. of Commerce.
- Niemczynowicz, J., 1986. The dynamic calibration of tipping bucket raingauges. *Nordic Hydrol.*, **17**, 203–214.
- Omre, H. and Halvorsen, K.B., 1989. The Bayesian bridge between simple and universal Kriging. *Math. Geol.*, **21**, 767–786.

- Pereira Filho, A.J. and Crawford, K.C., 1997. Integrating WSR-88D estimates and Oklahoma Mesonet measurements of rainfall accumulations: hydrologic response. In: *Weather radar technology for water resources management*, B. Braga Jr. and O. Massambani (Eds.). UNESCO Press, Paris, France. 419–454.
- Rosa Dias, Manuel P., 1994. Radar Measurements of precipitation for hydrological purposes. In: *Advances in radar hydrology*, M.E. Almeida-Teixeira, R. Fantechi, R. Moore and V.M. Silva (Eds.). European Commission Report EUR 14334 EN.
- Seo, D.J., Krajewski, W.F. and Bowles, D. S., 1990a. Stochastic interpolation of rainfall data from raingages and radar using cokriging. 1. Design of experiments, *Water Resour. Res.*, **26**, 469–477.
- Seo, D.J., Krajewski, W.F., Bowles, D. S. and Azimi-Zonooz, A., 1990b. Stochastic interpolation of rainfall data from raingages and radar using cokriging. 2. Results. *Water Resour. Res.*, **26**, 915–924.
- Seo, D.J. and Smith, J.A., 1991a. Rainfall estimation using raingages and radar. A Bayesian approach: 1. Derivation of estimators. *Stoch. Hydrol. Hydraul.*, **5**, 17–29.
- Seo, D.J. and Smith, J.A., 1991b. Rainfall estimation using raingages and radar. A Bayesian approach: 2. An application. *Stoch. Hydrol. Hydraul.*, **5**, 31–44.
- Uijlenhoet, R., van den Assem, S., Stricker, J.N.M., Wessels, H.R.A. and de Bruin, H.A.R., 1994. Comparison of areal rainfall estimates from unadjusted and adjusted radar data and raingauge networks. In: *Advances in radar Hydrology*, M.E. Almeida Teixeira, R. Fantechi, R. Moore and V.M. Silva (Eds.). European Commission, Report EUR 14334 EN. 84–104.
- WMO, 1981. *Guide to Hydrological Practices*, WMO publications, no. 168, 5th edition, Geneva, Switzerland.